Investigation of angular variations of radar sea clutter

Guerraou Zaynab[1,2] *Angelliaume Sébastien*[1] *Guérin Charles−Antoine*[2]

1: *ONERA, Département Electromagnétisme et Radar*

2: *Université de Toulon, Mediterranean Institute of Oceanography (MIO)*

ONERA ACTIVITIES – Sea surface radar imagery

Improving our knowledge of the EM scattered signal from the sea surface

- Target detection: Developing robust detection methods under difficult sea conditions (Detection of small targets, rough sea state…)
- Sea clutter: Modelling the EM sea surface response
- Detection/ characterization/ quantification of marine pollutants. (POLLUPROOOF project)
- Inversion of ocean surface parameters (wind/ wave heights/ ocean currents)

❑ Collaborative work:

- ❑ ONERA – Research labs (MIO, IETR , …)
- ❑ DEMR (multi-units/ multi-sites) : Modeling/ radar experimentation/ system expertise

CONTEXT OF THE STUDY

Various challenges :

- Modeling of the HH and HV returns
- The variability of the NRCS
- Breaking waves, sea spikes
- Azimuthal variations and directional asymmetries
- The directional wave number spectrum of the short waves
- Grazing angle configuration…

The purpose:

Recent progresses toward the depiction and simulation of some of these phenomena.

INGARA SYSTEM

Fully-polarimetric X band radar system maintained & operated within the « Defence Science & Technology Organisation »

Frequency	10.1 GHz
Grazing angles	15° à 45°
Range resolution	0.75 m
Cross-range resolution	62 m

INGARA radar and trial parameters (reproduced from [1])

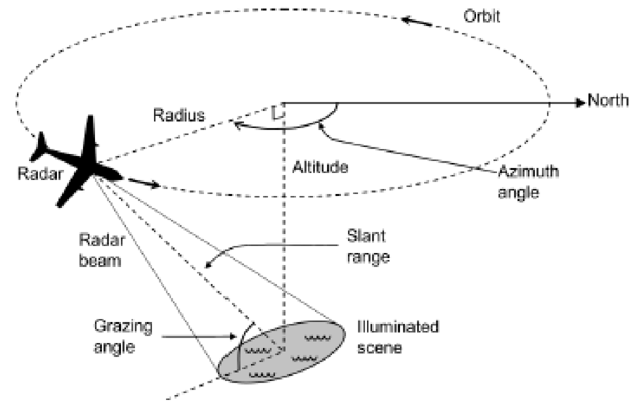

Circular spotlight mode collection for the INGARA data (reproduced from [1])

[1] Crisp, D.J., R. Kyprianou, L. Rosenberg, and N.J. Stacy, *Modelling the mean ocean backscatter coefficient in the plateau region at X-band.* Research report, DSTO, 2012.

INGARA SYSTEM

Fully-polarimetric X band radar system maintained & operated within the « Defence Science & Technology Organisation »

Frequency	10.1 GHz
Grazing angles	15° à 45°
Range resolution	0.75 m
Cross-range resolution	62 m

INGARA radar and trial parameters (reproduced from [1])

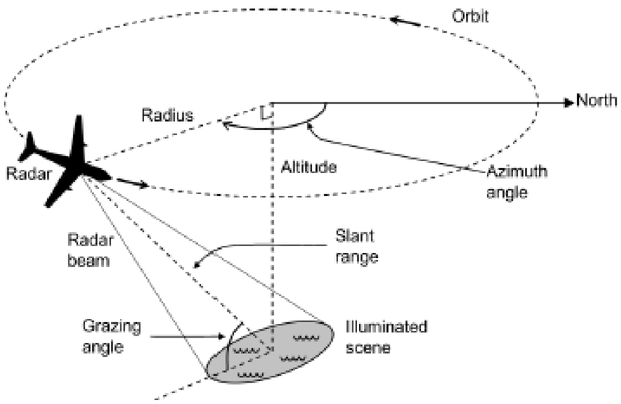

Circular spotlight mode collection for the INGARA data (reproduced from [1])

Trial	Flight	Date	Wind Speed (m/s)	Wind Direction (deg)	Wave Height (m)	Wave Direction (deg)	Wave Period (s)
SCT04	F33	9/8/04	10.2	248	4.9	220	12.3
SCT04	F34	10/8/04	7.9	248	3.5	205	11.8
SCT04	F35	11/8/04	10.3	315	2.6	210	10.4
SCT04	F36	12/8/04	13.6	0	3.2	293	8.8
SCT04	F37	16/8/04	9.3	68	2.5	169	9.7
SCT04	F39	20/8/04	9.5	315	3.0	234	11.4
SCT04	F40	24/8/04	13.2	22	3.8	254	12.2
SCT04	F42	27/8/04	8.5	0	4.3	243	12.5
MAST06	F2	17/5/06	8.5	115	0.62	112	3.1
MAST06	F4	19/5/06	3.6	66	0.25	35	2.6
MAST06	F8	23/5/06	3.5	83	0.41	46	4.0
MAST06	F9	24/5/06	10.2	124	1.21	128	4.6

Wind and wave ground truth for the Ingara data (reproduced from [1])

[1] Crisp, D.J., R. Kyprianou, L. Rosenberg, and N.J. Stacy, *Modelling the mean ocean backscatter coefficient in the plateau region at X-band.* Research report, DSTO, 2012.

Noise floor and denoising process

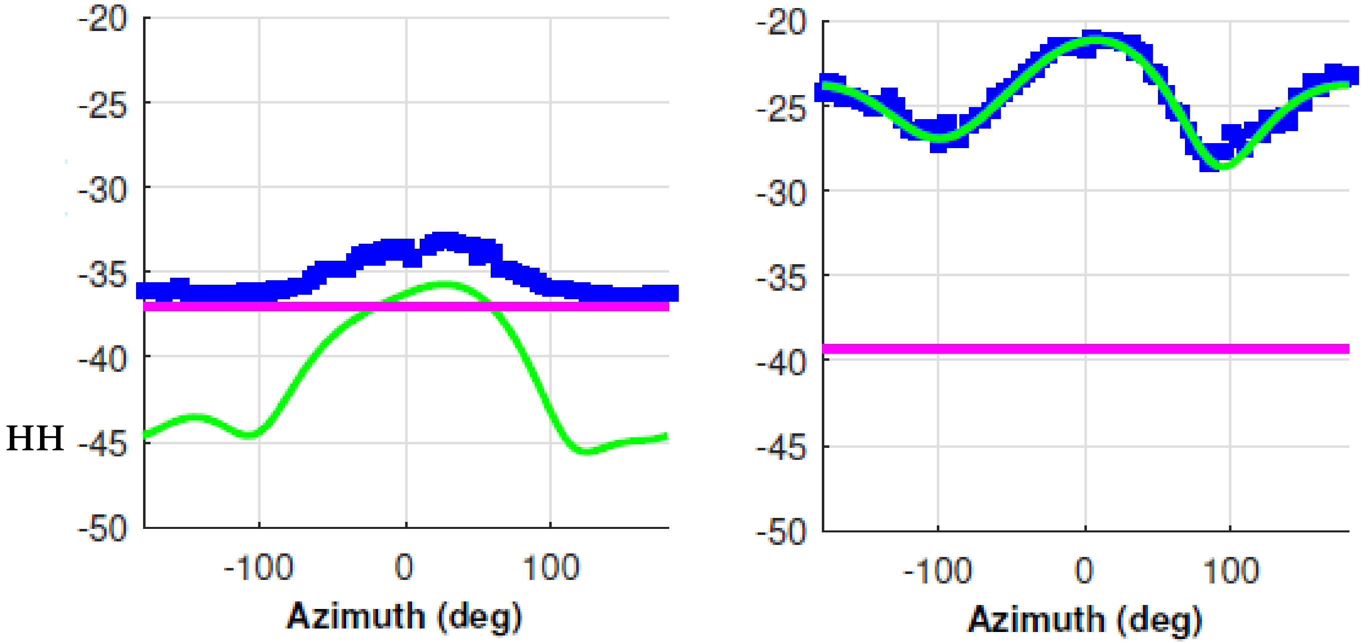

Azimuthal variation for HH polarized data for nominal grazing angles of 15° (left panel) and 45° (right panel) for a wind speed of 8.5 m/s

Raw NRCS
Mean noise estimate
Denoised NRCS

Upwind = 0°
Downwind = +/- 180°
Crosswind = +/- 90°

Azimuthal variation of the NRCS : *Maximum Likelihood estimation*

$$\sigma_0^{model}(\phi_n) = \tilde{\sigma}_0(\phi_n) + b(\phi_n)$$

Model: Truncated Fourier series $\tilde{\sigma}_0(\phi_n) = a_0 + \sum_{k=1}^{4} a_k \cos(k(\phi_n - \delta_k))$

Log-likelihood:

$$\mathcal{L} = -\frac{1}{2}\sum_{n=1}^{N_a} \log(2\pi\sigma_0^2) - \sum_{n=1}^{N_a} \frac{1}{2\sigma_b^2}\left[\sigma_0^{data}(\phi_n) - \left(\tilde{\sigma}_0(\phi_n) + \bar{b}\right)\right]^2$$

$$\frac{\partial\mathcal{L}}{\partial a_k} = 0\,,\ \frac{\partial\mathcal{L}}{\partial \phi_k} = 0 \ldots \quad \longrightarrow \quad a_n, \phi_n$$

Région PACA · mio Institut Méditerranéen d'Océanologie · ONERA THE FRENCH AEROSPACE LAB

Azimuthal variation of the NRCS :
HH peculiar behavior at low grazing angles

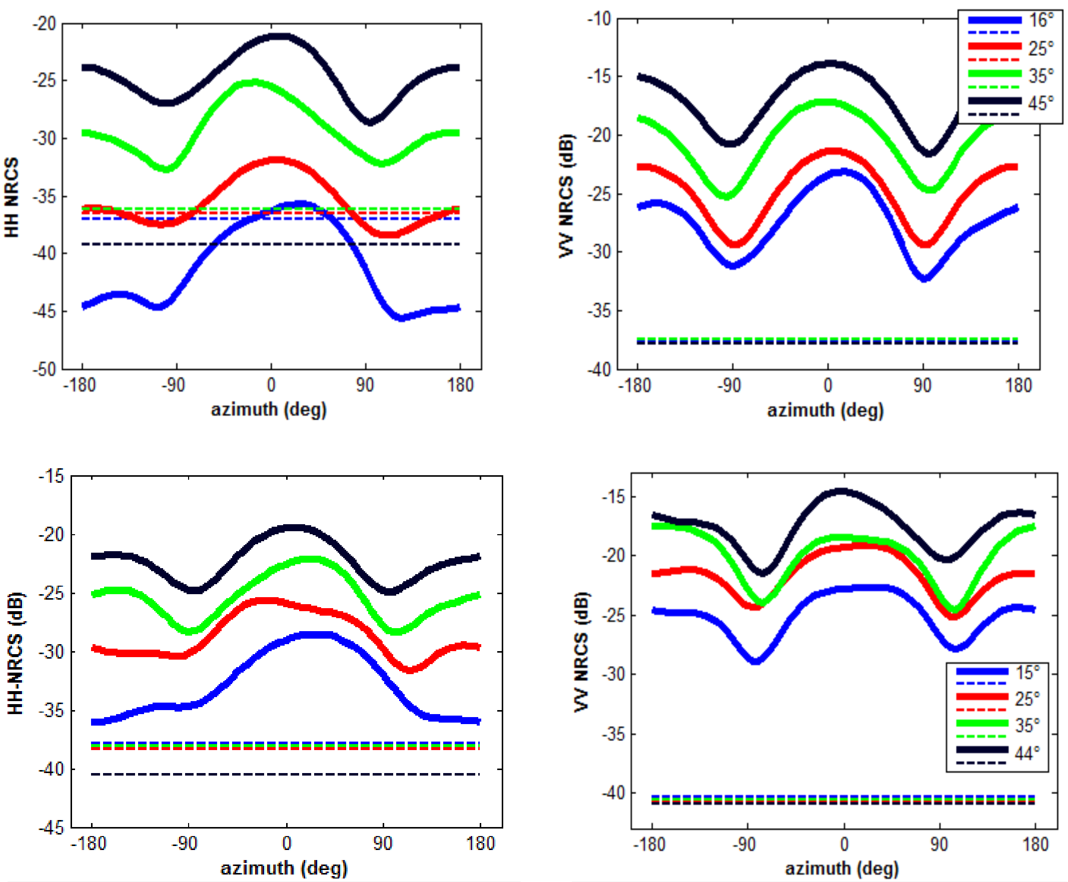

Azimuthal variation for HH and VV polarized data for nominal grazing angles for two different wind speeds (8.5 m/s for the upper panels and 10 m/s for the lower ones)

Progressive shift from two local maxima at upwind/downwind directions to a unique and pronounced maximum in the upwind direction

→ Physical interpretation?

Azimuthal variation of the NRCS : *Directional asymmetries*

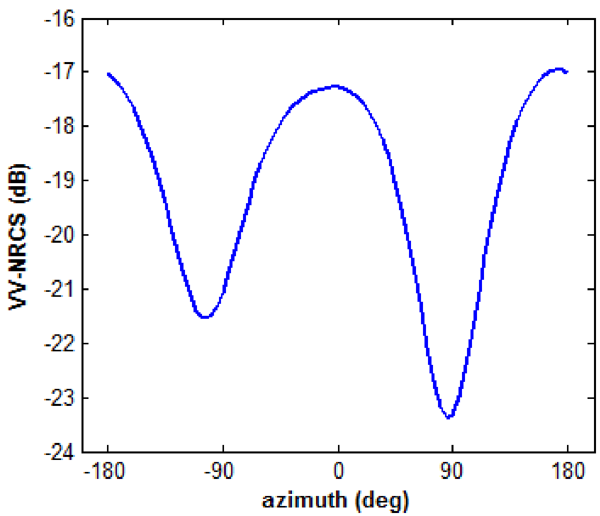

Example of the azimuthal variation for a 41° grazing angle, run3

- Upwind/Downwind asymmetry : $UDA = 10\ log10\left(\frac{\sigma^0_{up}}{\sigma^0_{down}}\right)$
- Upwind/Crosswind asymmetry : $UCA = 10\ log10\left(\frac{\sigma^0_{up}}{\sigma^0_{cross}}\right)$

Conclusions :

- UDA and UCA in VV and HH are maximum at moderate grazing angle (30° - 45°)
- $UDA_{HH} > UDA_{VV}$ & $UCA_{VV} > UCA_{HH}$(The maximum UDA in HH is in average about 2 dB higher than the VV counterpart.)

Relations between the different polarizations : *Polarization ratio – Grazing and azimuth behavior*

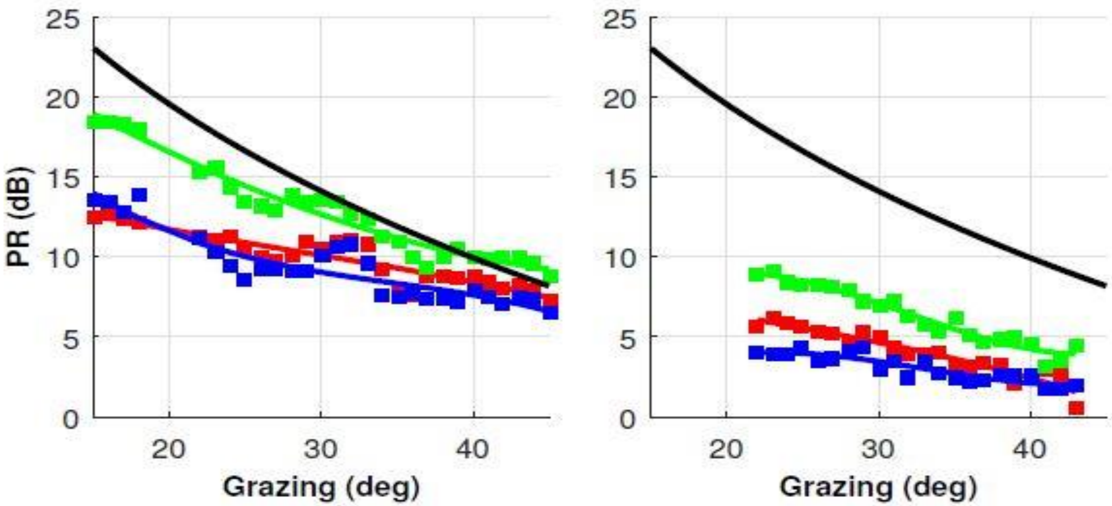

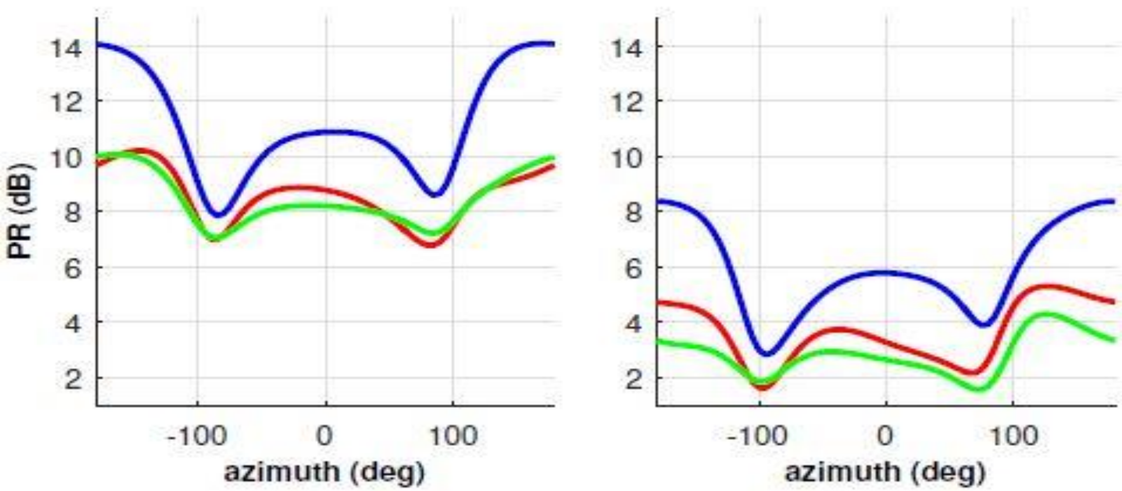

$$PR = (\sigma^0_{VV})_{dB} - (\sigma^0_{HH})_{dB}$$

Conclusions :

- The PR is a decreasing function of grazing angle
- $PR_{data} < PR_{Bragg}$
- PR has a strong azimuthal dependency with a sharp maximum in the downwind direction

Polarization ratio of asymmetric wave

Upwind & downwind

Polarization ratio using Bragg theory for a nominal incidence angle θ

$$\begin{cases} B_{VV} = \frac{\varepsilon-1}{(\varepsilon q_0+q_0')^2}\left(-{q_0'}^2 - \varepsilon k_0^2\right) \\ B_{HH} = \frac{\varepsilon-1}{(q_0+q_0')^2} K^2 \end{cases}$$

, With

$$\begin{cases} k_0 = K \sin\theta \\ q_0 = K \cos\theta \\ q_0' = \sqrt{\varepsilon K^2 - k_0^2} \end{cases}$$

$$\boldsymbol{PR_{Bragg}(\theta) = \frac{|B_{VV}|^2}{|B_{HH}|^2} = \frac{|q_0 + q_0'|^4}{|\varepsilon q_0 + q_0'|^4}\left[\sin^2\theta\ (1-\varepsilon) - \varepsilon\right]^2}$$

Région PACA mio ONERA THE FRENCH AEROSPACE LAB

Polarization ratio of asymmetric wave

Upwind & downwind

Polarization ratio using Bragg theory for a nominal incidence angle θ

$$\begin{cases} B_{VV} = \frac{\varepsilon-1}{(\varepsilon q_0+q_0')^2}\left(-{q_0'}^2 - \varepsilon k_0^2\right) \\ B_{HH} = \frac{\varepsilon-1}{(q_0+q_0')^2}K^2 \end{cases}$$

, With

$$\begin{cases} k_0 = K\, sin\theta \\ q_0 = K\, cos\theta \\ q_0' = \sqrt{\varepsilon K^2 - k_0^2} \end{cases}$$

$$\boldsymbol{PR_{Bragg}(\theta) = \frac{|B_{VV}|^2}{|B_{HH}|^2} = \frac{|q_0 + q_0'|^4}{|\varepsilon q_0 + q_0'|^4}\left[\sin^2\theta\ (1-\varepsilon) - \varepsilon\right]^2}$$

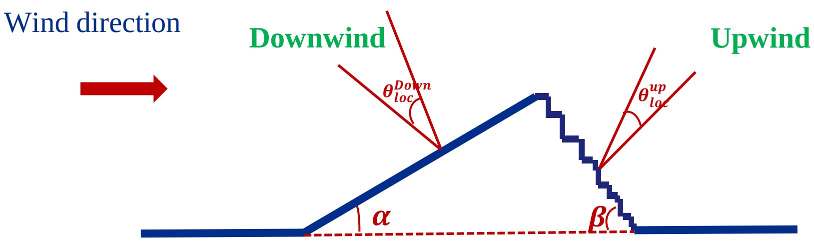

At local incidence angles:

$$PR_{loc} = PR(\theta_{loc}),\ \theta_{loc} = \begin{cases} \theta_i - \alpha & downwind \\ \theta_i - \beta & upwind \end{cases}$$

Polarization ratio of asymmetric wave
Upwind & downwind

Polarization ratio using Bragg theory for a nominal incidence angle θ

$$\begin{cases} B_{VV} = \frac{\varepsilon-1}{(\varepsilon q_0+q_0')^2}\left(-{q_0'}^2-\varepsilon k_0^2\right) \\ B_{HH} = \frac{\varepsilon-1}{(q_0+q_0')^2}K^2 \end{cases}, \text{ With } \begin{cases} k_0 = K\sin\theta \\ q_0 = K\cos\theta \\ q_0' = \sqrt{\varepsilon K^2-k_0^2} \end{cases}$$

$$\boldsymbol{PR_{Bragg}(\theta) = \frac{|B_{VV}|^2}{|B_{HH}|^2} = \frac{|q_0+q_0'|^4}{|\varepsilon q_0+q_0'|^4}\left[\sin^2\theta\,(1-\varepsilon)-\varepsilon\right]^2}$$

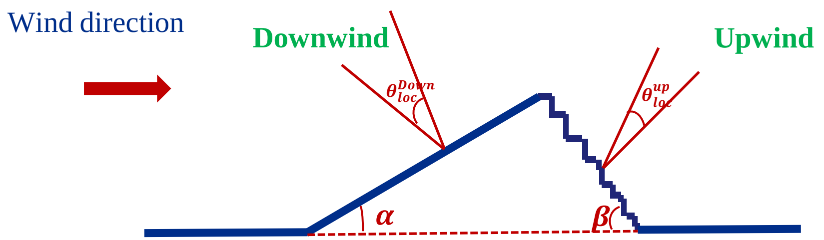

At local incidence angles:

$$PR_{loc} = PR(\theta_{loc}),\ \theta_{loc} = \begin{cases} \theta_i-\alpha & downwind \\ \theta_i-\beta & upwind \end{cases}$$

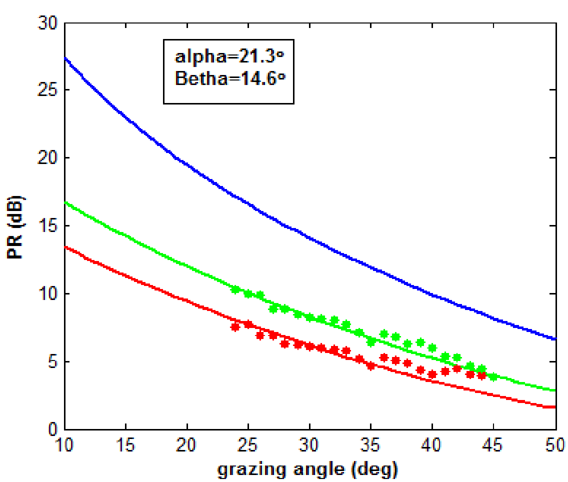

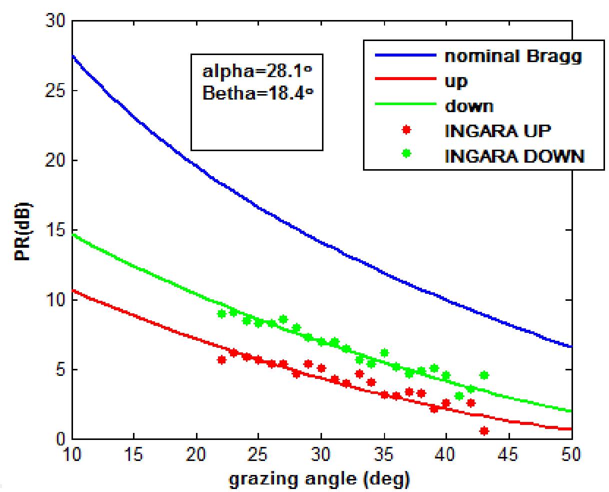

α and β angles are in good agreement with slopes obtained in wind-wave tank measurements (Cf Caulliez et al [2])

[2] Caulliez, G., and C.-A. Guerin (2012), Higher-order statistical analysis of short wind-waves, J. Geophys. Res., 117, C06002, doi:10.1029/2011JC007854.

Région PACA
mio
ONERA THE FRENCH AEROSPACE LAB

Relations between the different polarizations :

The polarization difference $\sigma^0_{VV} - \sigma^0_{HH}$

- $\sigma_0 = \sigma_0^p + \sigma_0^{np}$ (linear units)
- $\mathrm{P}D = \sigma^0_{VV} - \sigma^0_{HH}$ removes the non-polarized contribution

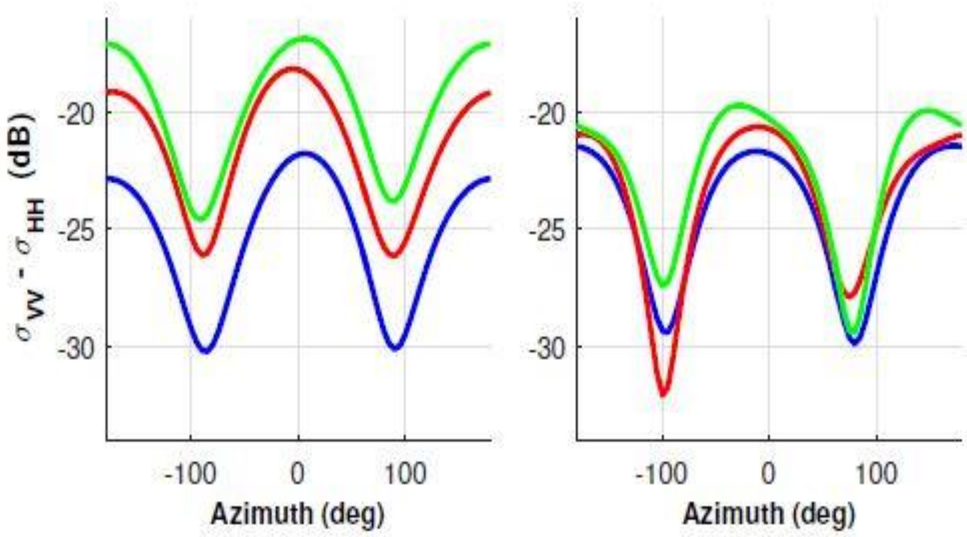

Grazing angles
25°
37°
42°

Azimuthal variation of the polarization difference VV-HH for run days 9 (left) and 12 (right)

No or **weak** UDA asymmetry!

Potential Interpration:

UDA asymmetry is likely to be contained in the non-polarized part and presumably related to the large scales of surface roughness?

Région PACA mio Institut Méditerranéen d'Océanologie ONERA THE FRENCH AEROSPACE LAB

Study of the cross-polarized data

Scattering models

- GOSSA [3] for the two-like polarizations
- SSA2 [4] for the cross-polarized data

Spectral models

Omni-directional spectra
- Elfouhaily [5]
- Bringer [6]

spreading functions
- Elfouhaily [5]
- Yurovskaya [7]

Azimuthal variation of the ratio

$$R = \frac{\sigma_{VH}^0}{\sigma_{VV}^0 - \sigma_{HH}^0} \propto mss_y$$

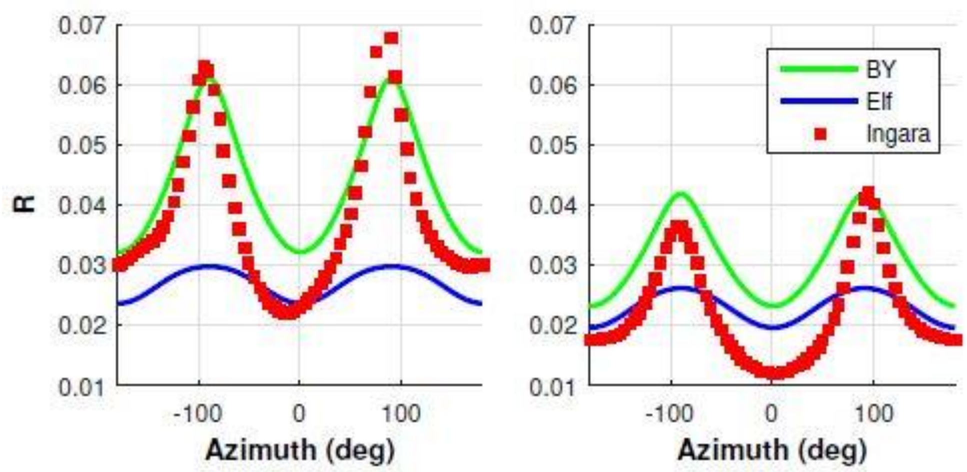

Azimuthal variation of the Ratio at 40° grazing angle for run days 3 (left) and 9 (right)

[3] G. Soriano and C.A. Gu´erin, "A cutoff invariant two-scale model in electromagnetic scattering from sea surfaces," Geoscience and Remote Sensing Letters, IEEE, vol. 5, no. 2, pp. 199–203, 2008.
[4] C.-A. Gu´erin and J.-T. Johnson, "A simplified formulation for the crosspolarized backscattering coefficient under the second-order small slope approximation," IEEE Trans. Geosci. and Remote Sens., 2015
[5] T. Elfouhaily and C.A. Guérin, "A critical survey of approximate scattering wave theories from random rough surfaces," Waves in Random and Complex Media, 2004.
[6] A. Bringer, B. Chapron, A. Mouche, and C.-A. Guérin,"Revisiting the short-wave spectrum of the sea surface in the light of the weighted curvature approximation," IEEE Trans. Geosci. and Remote Sens.,2014.
[7] MV Yurovskaya, VA Dulov, Bertrand Chapron, and VN Kudryavtsev, "Directional short wind wave spectra derived from the sea surface photography," Journal of Geophysical Research: Oceans, 2013.

Simultaneous variation of the different polarizations

- Systematic correlation between the *HH* & *HV* polarizations ($\rho > 0.9$)
- Poorer correlation between the VV and HV channels ($\rho < 0.8$), albeit following the same trend

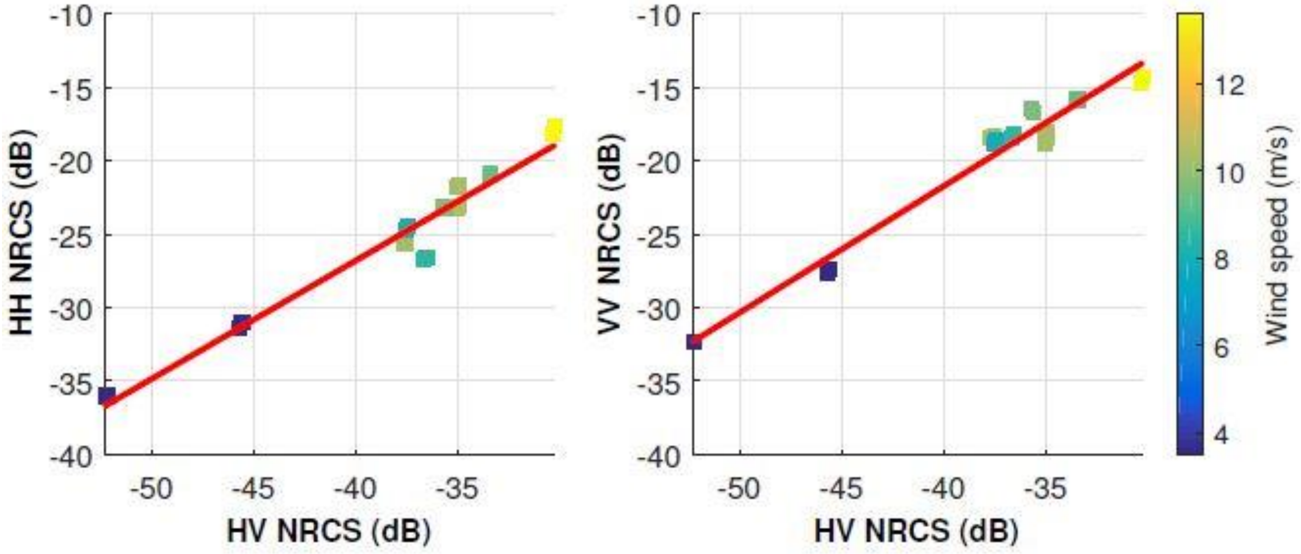

Scatterplot of HH versus HV (left) and VV versus HV (right) for the mean NRCS taken at 37 degrees grazing angle within ± 2.5 degrees from the upwind direction with linear fit shown in red.

HH & VV NRCS

Significant improvement of the simulated HH and VV NRCS brought by the use of the improved spectral models

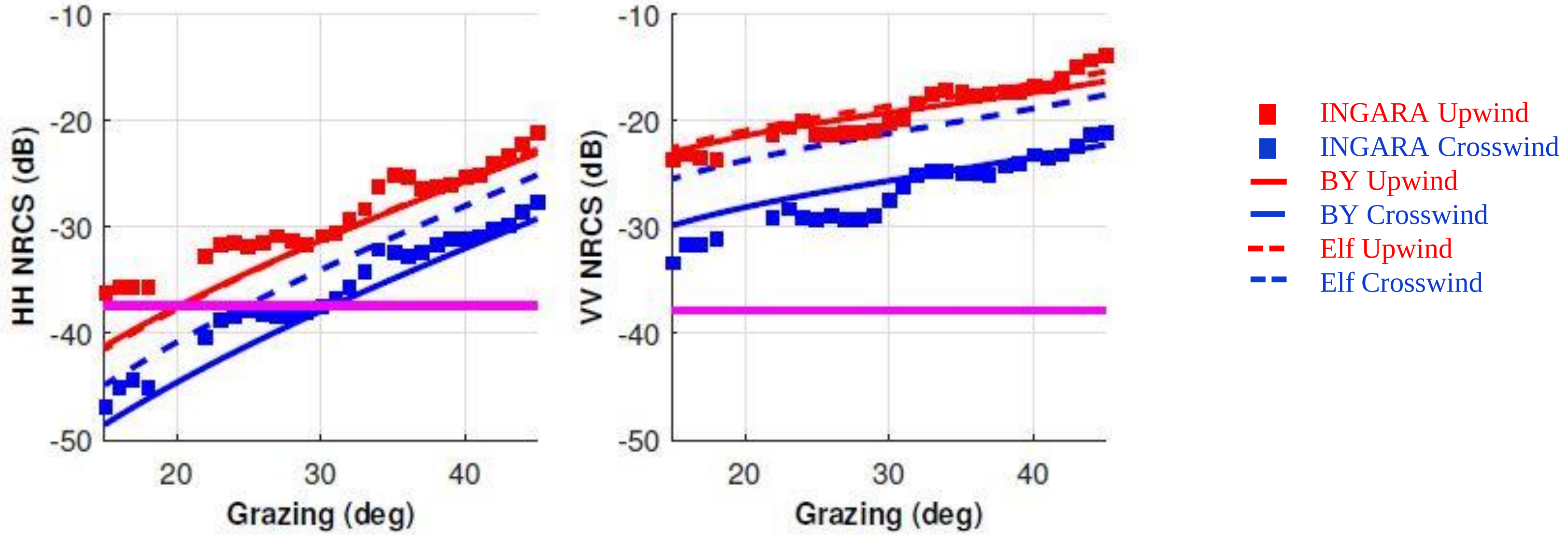

HH (left) and VV (right) NRCS from the INGARA MGA data for run day 9. Superimposed is the simulated NRCS according to the GO-SSA model with Elfouhaily directional spectrumand Bringer-Yurovskaya model.

Conclusion

- Peciluar azimuthal distribution at low grazing angles for HH-polarized data
- UDA & UCA asymmetries are not monotone functions of grazing angle and reach their maximum at moderate grazing angles (30°-45°)
- $UDA_{HH} > UDA_{VV}$ & $UCA_{VV} > UCA_{HH}$
- PR max at downwind
- $\frac{\sigma^0_{VH}}{\sigma^0_{VV}-\sigma^0_{HH}}$ maximum at crosswind and no or weak UDA for the $\sigma^0_{VV} - \sigma^0_{HH}$
- Eventual correlation between HH and HV polarized data
- Improvement of the co-polarized simulated NRCS brought by the use of improved spectral models

THANK YOU FOR YOUR ATTENTION

QUESTIONS?

Azimuthal variation of the NRCS : *Maximum Likelihood estimation*

Robustness of the MLE to the SNR degradation

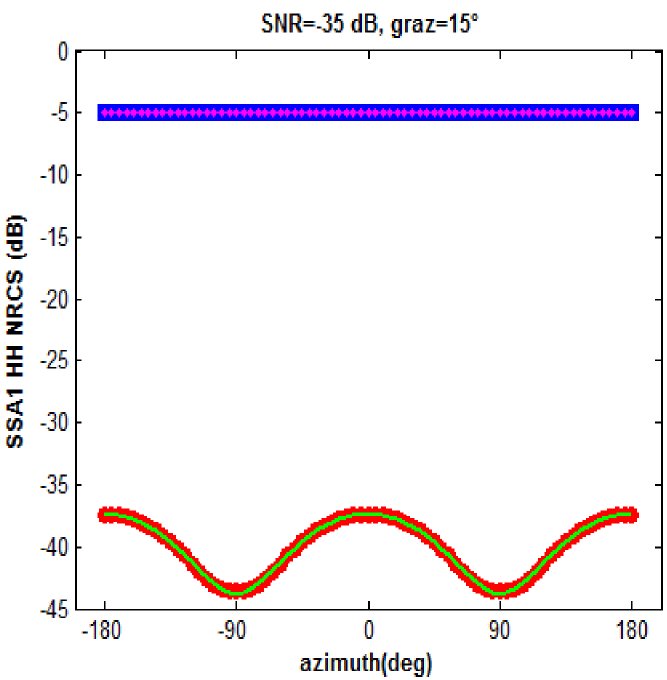

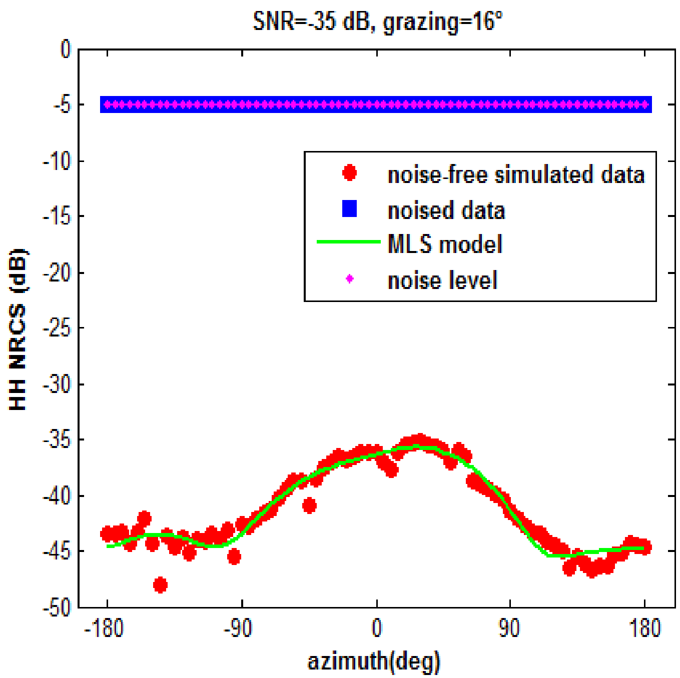

The RMSE calculated between the noise-free simulated data and the estimated model is found to be significantly low and quite insensitive to the SNR.

Example of NRCS reconstruction at low SNR of -35 dB

Région PACA mio ONERA THE FRENCH AEROSPACE LAB

Effect of swell

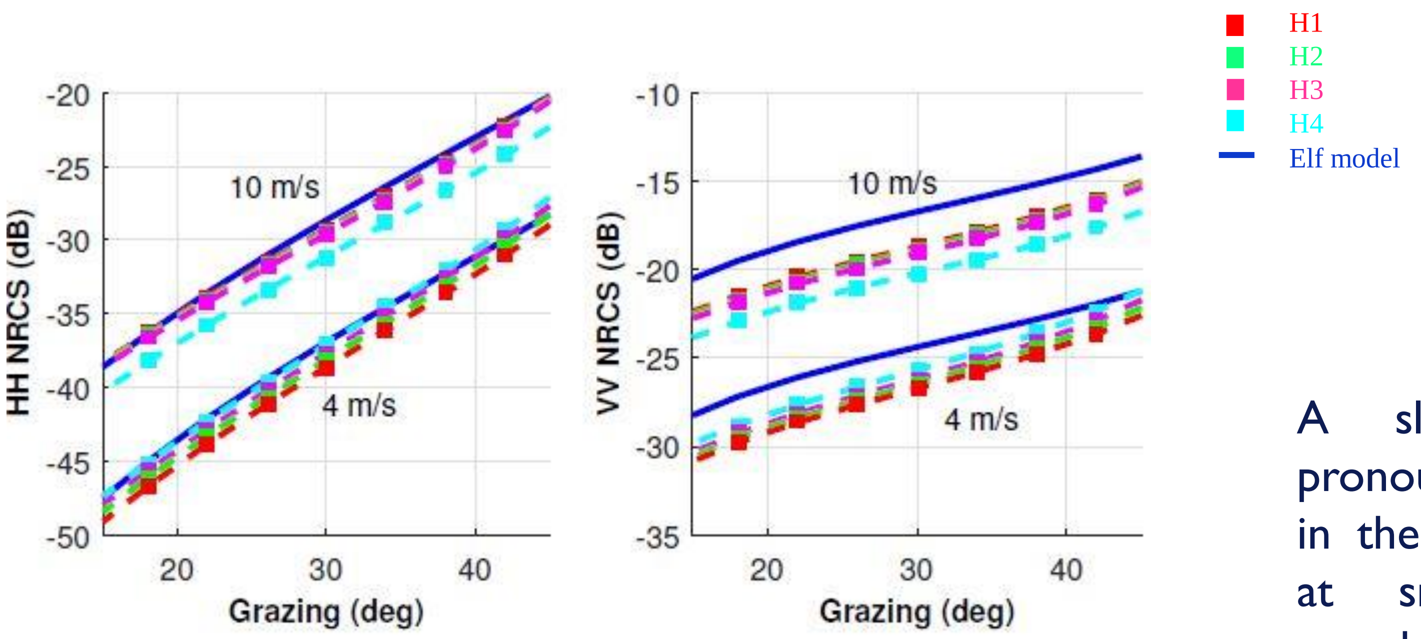

VV(upper dots) and HH (lower dots) NRCS for the Hwang spectrum with different swell indices for a 4m/s wind speed on the left panel and 10m/s on the right panel

A slightly more pronounced effect in the HH pol and at smaller wind speeds